JCB

Supplemental material

Kumar et al., **https://doi.org/10.1083/jcb.201903102**

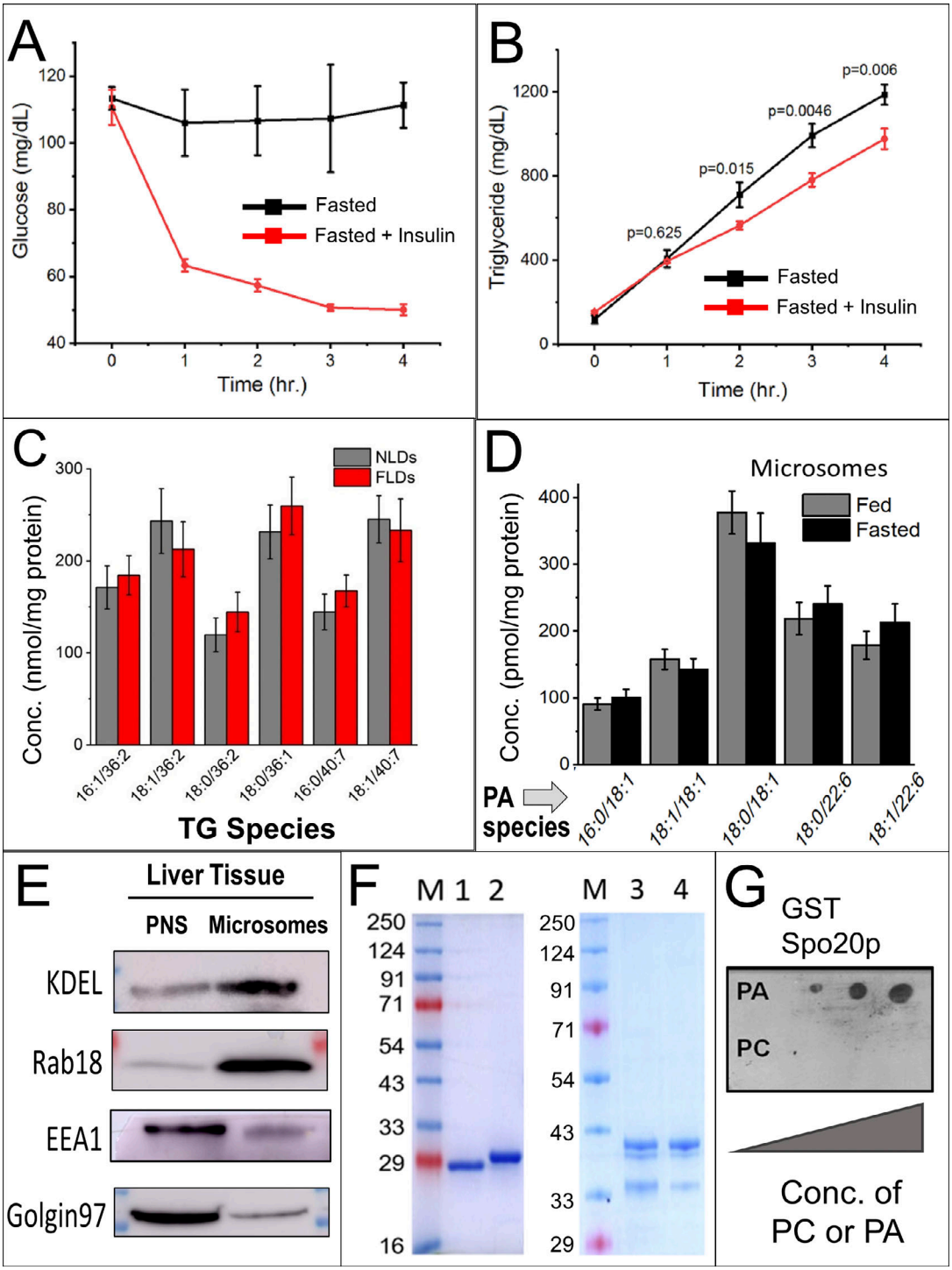

Figure S1. **Effect of insulin on glucose and TG levels of fasted rats and related experiments. (A)** Fasted rats were injected with saline (fasted control) or 0.75 IU insulin (fasted + insulin). Glucose level was measured in the blood collected at 1-h intervals for 4 h. The experiment was conducted independently on three pairs of animals. The data represent mean ± SD. **(B)** Triglyceride levels were measured in the blood collected from animals treated as in A. The experiment was conducted independently on three pairs of animals. The data represent mean ± SD. **(C)** TG species (FA chain lengths indicated) in NLDs and FLDs were quantified by lipidomic analysis. The samples were normalized on the basis of proteins stripped from LDs. The experiment was conducted independently with five pairs of animals. The data represent mean ± SEM. Conc, concentration. **(D)** Microsomal membrane fractions were prepared from fed and 16-h-fasted animals. PA level was measured by quantitative lipidomics. The samples were normalized using total proteins stripped from the samples. There was no significant change in the PA. The data represent mean ± SEM. **(E)** Purity of microsomes prepared from rat liver. ER markers (KDEL and Rab18) are enriched on microsomes, but endosome marker (EEA1) and Golgi marker (Golgi97) are barely detectable. **(F)** GST-tagged proteins were purified from bacteria, and purity was estimated by SDS-PAGE gels stained with Coomassie dye. M, marker; lane 1, GST; lane 2, GST-Spo20p (PA-sensor); lane 3, GST-kinesin tail domain (GST-KTD); lane 4, GST-KTD(PA^-). **(G)** The PA sensor protein GST-Spo20p was overlaid on nitrocellulose membrane spotted with varying concentrations (50, 200, 1,000 pmol) of PC and PA. The membrane was immunoblotted with GST antibody. GST-Spo20p binds with PA in a dose-dependent manner, but not with PC.

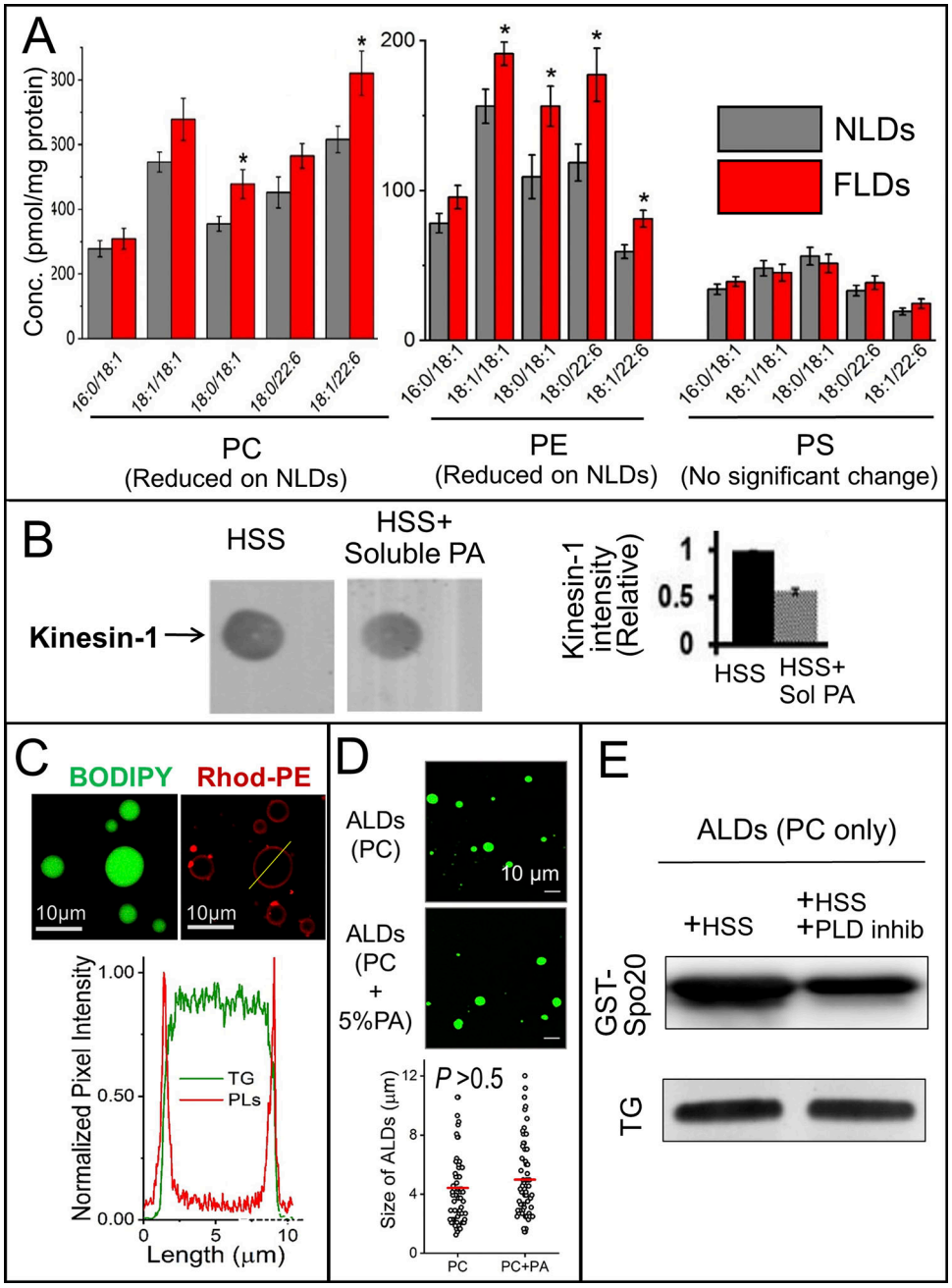

Figure S2. **LC-MS of phospholipid species on LDs, effect of soluble PA on kinesin binding, and related experiments using artificial LDs (ALDs). (A)** Phospholipids on NLDs and FLDs measured by quantitative lipidomics. The samples were normalized by total proteins stripped from LDs. The data represent mean ± SEM for five biological replicates. *, P < 0.05. Two-tailed *t* test used. Data distribution was assumed to be normal, but this was not formally tested. Conc, concentration. **(B)** Lipid blot assay with 2.5 nM PA spotted on nitrocellulose membrane. BRL3A PNS (mock or treated with soluble PA) was overlaid on the membrane. The membrane was immunoblotted against kinesin-1 antibody. Kinesin-1 binding to PA is reduced after soluble PA treatment. Error bars are SEM. **(C)** ALDs were synthesized using TG, PC, and Rhodamine-PE. TG containing core was stained with BODIPY. The line intensity profile shows a TG-containing core covered by phospholipid monolayer. **(D)** Size of ALDs synthesized with PC and PC + 5% PA shows no significant difference. Scatter plot represents diameters of 60 randomly selected ALDs in each condition; horizontal red line indicates mean value; *, P > 0.5. **(E)** PC-only ALDs were incubated with liver HSS, and then separated to estimate generation of PA on the ALDs. Significantly less PA-sensor (GST-Spo20p) binds to ALDs in the presence of PLD inhibitor (inhib). Equal loading of ALDs is confirmed by thin layer chromatograph for TG. The blot is representative of three independent experiments.

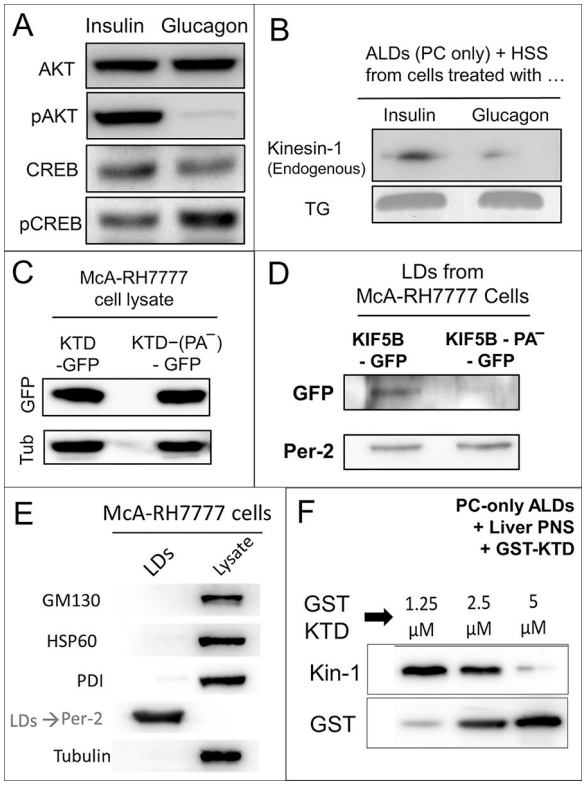

Figure S3. **Effect of insulin, glucagon treatment, and kinesin tail domain expression. (A)** Western blot to verify the effect of insulin and glucagon treatment on McA-RH7777 cells. Insulin and glucagon pathways are known to phosphorylate AKT and CREB, respectively. Accordingly, pAKT is detected in insulin-treated cells and pCREB in glucagon-treated cells. **(B)** HSS (devoid of membrane, organelles, and endogenous LDs) was prepared from insulin- or glucagon-treated McA-RH7777 cells. HSS was incubated with ALDs synthesized using PC and TG. The ALDs were separated by flotation and immunoblotted with kinesin-1 antibody. TLC for TG was performed to confirm equal loading of ALDs. **(C)** McA-RH7777 cells stably expressing KTD-GFP and KTD(PA⁻)-GFP were used to prepare crude cell lysate. Immunoblotting of lysate was performed using antibodies against GFP and tubulin (loading control). Equal expression of the two GFP-tagged proteins is observed. **(D)** LDs were purified from McA-RH7777 cells stably expressing full-length KIF5B-GFP and KIF5B(PA⁻)-GFP. Proteins bound to LDs were immunoblotted with GFP and perilipin-2 (Per-2) antibodies. KIF5B-GFP shows stronger binding to LDs in comparison to KIF5B(PA⁻)-GFP. Equal loading of LDs is confirmed by Per-2 band. **(E)** Purity of LDs isolated from McA-RH7777 cells. LDs were isolated by floatation from cells loaded with 400 µM OA for 12 h. Western blotting performed on LDs and cell lysate shows enrichment of perilipin-2 (LD marker) on LDs, while other organelle specific markers GM130 (Golgi complex), HSP60 (mitochondria), PDI (microsome), and tubulin (cytoskeleton) were not detected on the LD fraction. **(F)** ALDs (only PC) were incubated with liver HSS to recruit proteins (e.g., kinesin-1) onto ALDs, separated, and divided into three equal parts. These ALDs were then incubated with purified GST-KTD at the concentrations indicated. ALDs were again separated by centrifugation, and Western blotting was performed using kinesin-1 and GST antibodies. GST-KTD displaces kinesin-1 from ALD membrane in a dose-dependent manner.

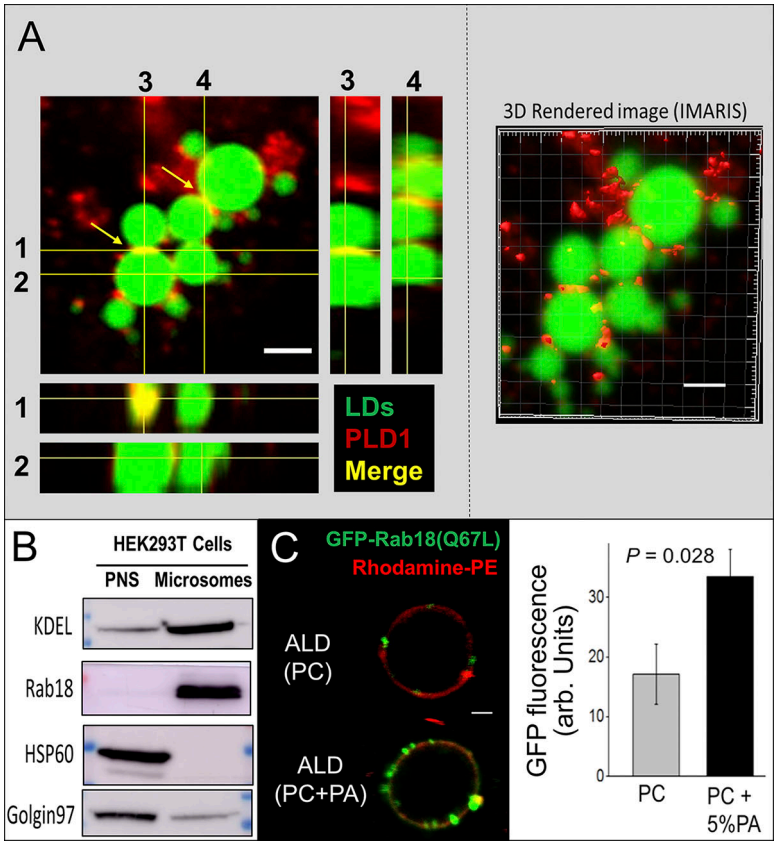

Figure S4. **Role of phosphatidic acid in protein exchange between LDs and ER. (A)** McA-RH7777 cells were immunostained with PLD1 specific antibody; LDs were stained with MDH and imaged on laser-scanning confocal microscope. Arrows indicate staining of PLD1 at LD–LD contacts. Z-plane sections through the LD–LD contacts and LD center taken at four different positions are shown as XZ and YZ orthogonal projections. PLD1 is specifically localized at the LD–LD contact zones. Scale bar = 2 µm. Right panel shows a 3D rendition of the confocal image prepared using IMARIS software. Scale bar = 2 µm. **(B)** Purity of microsomes prepared from HEK 293T cells. Western blot of microsomes shows enrichment of KDEL (ER marker) and Rab18. HSP60 (mitochondrial marker) and Golgin97 are barely detectable on microsomes. **(C)** Microsomes prepared from HEK-293T cells overexpressing GFP-Rab18(Q67L) (a GTP-mimic) were incubated with ALDs synthesized using PC or (PC + 5% PA). Both ALDs were supplemented with 0.1% rhodamine-PE for visualization. ALDs were separated by flotation and imaged on a confocal microscope. A representative ALD is shown for each case. Significantly more GFP-Rab18 is recruited on PA-containing ALDs. Scale bar = 1 µm. Right panel shows quantification of fluorescence on the ALD surface using 8–10 LDs in each condition. Two tailed *t* test used. Data distribution was assumed to be normal, but this was not formally tested. arb, arbitrary. Error bars are SEM.